Characterization with embedded synchronization for read-write channels

Characterization with Embedded Synchronization for Read–Write Channels

Maria Yu Lin, J. W. M. Bergmans, George Mathew, and Say Wei Foo

***Abstract*—As densities and data rates increase, accurate characterization of the read/write process becomes increasingly critical in magnetic/optical recording. In this paper, we propose an advanced synchronous characterization scheme which employs joint synchronization and characterization in data-aided mode. This is a completely adaptive approach with distinct features which make it superior to existing characterization techniques. It can work with arbitrary data patterns and it is suitable for characterizing both magnetic and optical channels. Further, because it is operating in data-aided mode, it can tolerate much larger noise and distortions compared to a nondata-aided approach. Hence, the proposed approach is well suited for read–write channels with high densities, high data-rates, and/or low signal to noise ratios.**

***Index Terms*—Adaptive resampler, joint synchronization and characterization, magnetic recording, optical recording, phase lock loop (PLL), synchronous characterization.**

I. Introduction

As densities and data rates increase, accurate characterization of the read/write process becomes increasingly critical in magnetic and optical recording applications. It is important to develop characterization techniques which are robust enough to work satisfactorily in the presence of different kinds of distortions that arise at high recording densities, high data-rates, and/or low signal to noise ratios (SNR). It is also desirable that the characterization techniques be flexible enough to accommodate different channel models and code constraints, so as to represent normal recording conditions. The existing characterization techniques can be classified into asynchronous and synchronous techniques. Asynchronous techniques, such as dipulse extraction [1], generally estimate specific channel parameters using a fixed data pattern which may not represent normal recording conditions. On the other hand, synchronous techniques, such as those in [2], construct more complete channel models and are suitable for a variety of data patterns. However, the existing synchronous techniques use a separate synchronizer, which may work poorly or break down under difficult recording conditions.

In this paper, we propose a characterization scheme with embedded synchronization that overcomes these drawbacks. Section II presents the architecture of the proposed approach and highlights its main advantages. Section III presents the details of the synchronization algorithm. Section IV presents results, obtained using measured and simulated signals, demonstrating the efficacy of the proposed approach.

Manuscript received October 16, 2000.

M. Y. Lin and G. Mathew are with the Coding and Signal Processing Department, Data Storage Institute, Singapore (e-mail: marialin@dsi.nus.edu.sg).

J. W. M. Bergmans is with Eindhoven Technological University, The Netherlands.

S. W. Foo is with the National University of Singapore.

Publisher Item Identifier S 0018-9464(01)06663-8.

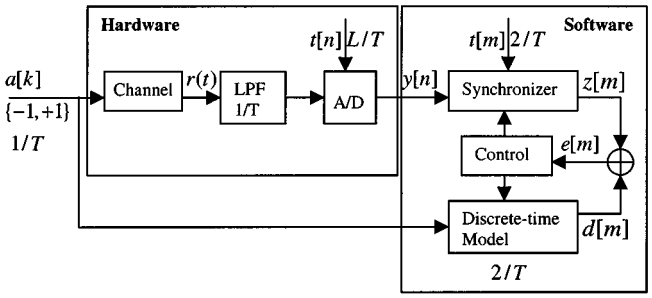

Fig. 1. Block schematic of the synchronous characterization system.

II. Architecture of the Synchronous Characterization Scheme

Fig. 1 shows the architecture of the synchronous characterization scheme proposed in this paper. Here, $a[k]$ is the input binary data in $\{-1, +1\}$ format, T is the duration of one bit, and L is the over-sampling factor. The time indices k, m and n are associated with sampling rates $1/T$, $2/T$ and L/T, respectively. The channel path consists of a physical channel (the read/write process), an anti-alias low pass filter (LPF), and an A/D converter. The LPF is meant to eliminate any noise outside the pass-band of the signal. The signal $y[n]$ after the A/D converter is asynchronous to the input $a[k]$. The discrete-time channel model is initialized with reasonable parameter values, and its output is fully synchronous to $a[k]$. The synchronizer converts the asynchronous signal $y[n]$ into $z[m]$ that is synchronous with $a[k]$. The control block fine-tunes the model adaptively. A pre-processor, not shown here, conditions the readback signal against undesirable offsets and gains, and checks for anomalies that could upset the characterization process.

As shown, the synchronization and characterization loops operate jointly in a data-aided fashion based on the same error signal. This leads to high accuracy in the model and synchronization. This is a completely adaptive approach and it can work with wide variety of data patterns, code constraints, and channel models. This makes it suitable for use in characterization of magnetic and optical channels. The characterization loop fine-tunes the channel model and removes the data dependent distortions adaptively. This reduces the influence of these distortions on synchronization. Furthermore, the existing synchronous techniques use a separate synchronizer that operates either in decision-directed mode or based on simple alignment techniques. In comparison, our approach is a

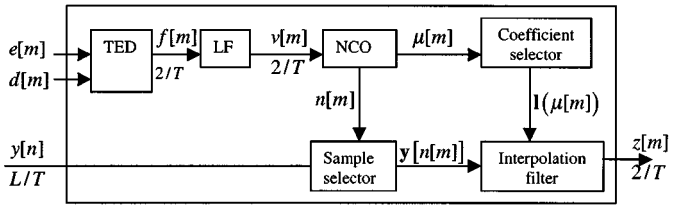

Fig. 2. Detailed schematic of synchronizer.

data-aided approach that uses full knowledge of the input data. Therefore its performance will not be influenced by erroneous decisions, and is more accurate and robust. Thus it is suitable for use under difficult conditions, such as high densities, high data-rates and/or low SNRs.

III. Synchronizer

The synchronizer consists of a coarse synchronizer and a fine synchronizer. The coarse synchronizer synchronizes the initial portions of $y[n]$ and $a[k]$ to within one symbol interval by cross-correlating the model output (using a reasonable initial model) with the read-back signal.

Fig. 2 shows the details of the fine synchronizer which consists of a timing error detector (TED), a loop filter (LF) and a numerically controlled oscillator (NCO). The TED estimates the phase difference between the model output $d[m]$ and the resampled channel output $z[m]$. The LF filters the noisy estimates $f[m]$ from the TED. The NCO generates the next sampling instant $t[m]$ based on the output $v[m]$ of LF. The sample selector, coefficient selector and interpolation filter resample the oversampled readback signal $y[n]$ according to $t[m]$. All these elements together form a control loop, which accurately synchronizes the replay signal (to within a small fraction of T), by minimizing the phase error estimated by the TED. Therefore, it is important to have a TED whose timing function, $\rho(\Delta) = E[f[m]]$, has the following properties: $\rho(\Delta = 0) = 0$ and $sign[\rho(\Delta)] = sign(\Delta)$, where Δ is the phase error between $z[m]$ and $d[m]$. The channel model, which could be linear or nonlinear, is adaptively updated while the timing loop is running, using the least mean square (LMS) algorithm or its derivatives (see [3, Ch. 8]).

To reduce the complexity of the LPF and the interpolation filter, and to ensure no loss of any signal, the channel is sampled at twice the bit-rate for doing synchronization and characterization. For simplifying the analysis, we assume a linear channel with impulse response $h(t)$ and additive noise $n(t)$ at the output, and a linear model with impulse response $c[m]$. Assuming that the resampler is frequency-synchronous to $2/T$ so that the output $z[m]$ only exhibits a phase error with respect to $d[m]$, we can denote the resampling instants as $t[m] = mT/2 + \Delta \cdot T$ where Δ denotes the normalized (by T) sampling-phase error. Then, we can write the resampler output, model output, and error signal $e[m] = z[m] - d[m]$ as

$$z[m] = \sum_k a[k]q[m - 2k] + u[m]$$

$$d[m] = \sum_k a[k]c[m - 2k]$$

$$e[m] = \sum_k a[k](q[m - 2k] - c[m - 2k]) + u[m]$$

respectively, where $q[m] = h(mT/2 + \Delta \cdot T)$ and $u[m]$ denotes the filtered and sampled noise. Note that $q[m]$ depends on Δ.

A. Timing Error Detector

We present a TED that satisfies the desired properties mentioned above for both magnetic and optical channels. Timing recovery is based on a zero-forcing approach, i.e., forcing the correlation between the error $e[m]$ and the differentiated version of the model output $d[m]$ to zero [3]. Thus, the TED output is given by

$$f[m] = e[m](d * w)[m] \tag{1}$$

where $w[m]$ approximates the differentiator. We have chosen, $w(D) = D^{-1} - D$ where D denotes one-sample delay ($T/2$ seconds), and $*$ denotes convolution. To keep the analysis simple, we assume uncorrelated random data $a[k]$. Using this, we get

$$\rho(\Delta) = \sum_i (q[i] - c[i])(w * c)[i]. \tag{2}$$

Suppose that $c[i]$ is odd-symmetric ($c[-i] = -c[i]$), as in the magnetic recording case. Since $w[m]$ is also odd-symmetric, $(c^* w)[i]$ will be even-symmetric ($(c * w)[i] = (c * w)[-i]$) resulting in $\sum_i c(i)(w * c)[i] = 0$. Thus,

$$\rho(\Delta) = \sum_i q[i](w * c)[i]. \tag{3}$$

If $q[i]$ is odd-symmetric for $\Delta = 0$, then $\rho(\Delta = 0) = 0$, and $sign[\rho(\Delta)] = sign(\Delta)$. Hence, the loop will settle at $\Delta = 0$. Using similar arguments, it is easy to see that in the case where $c[i]$ and $q[i]$ are even-symmetric (as in optical recording), the loop will settle at $\Delta = 0$.

B. Adaptive Resampler: Interpolator

As noted above, the resampler converts the input $y[n]$ which is at the rate L/T to the output $z[m]$ at the rate $2/T$. The resampling instants $t[m]$ may be expressed in terms of the time base at the resampler input as

$$t[m] = (n[m] + \mu[m])T_y$$

where $T_y = T/L$, $n[m]$ is an integer that is referred to as the basepoint index and $\mu[m]$ is a fraction ($0 \leq \mu < 1$) that is referred to as the fractional interval. Using this notation, we may express the resampler output as

$$z[m] = (y * l(\mu[m]))\,[n[m]]. \tag{4}$$

Here, $*$ denotes convolution and $l(\mu[m])$ is the impulse response of the interpolation filter (transversal filter with $T/2$-spaced taps) for the fractional interval $\mu[m]$. The sample selector is a shift register that shifts $n[m] - n[m-1]$ locations to the right at instant m. The coefficients of the interpolation filter are re-loaded every sampling instant m, depending on the fractional interval $\mu[m]$. Since the simple case of linear interpolation may

not be accurate enough, we use a 5-point Lagrange interpolator with coefficients given by

$$l_{-2} = (\mu[m]+1) * \mu[m] * (\mu[m]-1) * (\mu[m]-2)/24;$$
$$l_{-1} = -(\mu[m]+2) * \mu[m] * (\mu[m]-1) * (\mu[m]-2)/6;$$
$$l_0 = (\mu[m]+2) * (\mu[m]+1) * (\mu[m]-1) * (\mu[m]-2)/4;$$
$$l_1 = -(\mu[m]+2) * (\mu[m]+1) * \mu[m] * (\mu[m]-2)/6;$$
$$l_2 = (\mu[m]+2) * (\mu[m]+1) * \mu[m] * (\mu[m]-1)/24.$$

The interpolation filter could be redesigned to minimize the mean-square value of the interpolation error. This would be required if the oversampling ratio $L < 2$.

C. Numerically Controlled Oscillator (NCO)

For each sampling instant $t[m]$, the NCO computes the corresponding basepoint index $n[m]$ and fractional interval $\mu[m]$. This is done recursively according to

$$n[m] = n[m-1] + floor(p[m]/T_y + \mu[m-1]) \quad (5)$$
$$\mu[m] = (\mu[m-1] + P[m]/T_y) \bmod 1 \quad (6)$$

where $floor(x)$ represents the largest integer not exceeding x and $p[m] = t[m+1] - t[m]$ is the mth sampling period. $p[m]$ is derived from the output of the loop filter as $p[m] = (1 + v[m])2/T$.

D. Loop Filter and PLL Properties

We use a proportional-plus-integral type loop filter [3] with transfer function $V(z)/F(z) = K_p + (K_f/z - 1)$ where K_p and K_f are the gains along the phase and frequency branches, respectively. Since the transfer function of NCO is $T(z)/P(z) = 1/(z-1)$, the overall system from loop filter input to NCO output, i.e., $T(z)/F(z)$, is a second order discrete-time control system, whose properties can be found in [3, Ch. 11]. The loop filter should be properly dimensioned in relation to the sensitivity of the TED in order for the loop to have prescribed damping factor $\zeta = \sqrt{K_d K_f}$ and natural frequency $\omega_n T/2 = K_d K_p/(2\sqrt{K_d K_f})$. Since this requires knowledge of K_d, which is not accurately known beforehand, we may initially set-up the loop as a first order PLL (i.e., $K_f = 0$) and estimate the value of K_d by measuring the time-constant which is given by $1/(K_d K_p)$.

IV. Results and Conclusion

In this section, we give two examples of joint synchronization and characterization to illustrate that the proposed approach can work well under extremely difficult recording conditions. The first example uses the readback signal measured from a spin-stand at channel density 4.9 without any write-precompensation. The channel model used in this case is a linear filter $c[m]$ followed by the nonlinear transfer function $g(x) = \alpha_2 x^2 + x + \alpha_0$, where $c[m]$, α_0 and α_2, are the parameters to be identified. The second example uses simulated readback signal at density 3.0 with data dependent transition-shifts in the range $\{-0.4T, 0.4T\}$. The channel model used in this case is the Volterra model given in [2]. Figs. 3 and 4 show the readback signal (solid line) and model output (dashed line) in the beginning and steady-state portions of the data-blocks. Observe that the synchronization is only approximate in the beginning [Figs. 3(a) and 4(a)] since the model parameters are far from their optimum. However, as the model converges [Figs. 3(b) and 4(b)], the synchronization becomes accurate. The mis-match observed in Fig. 3(b) compared to Fig. 4(b) is due to the fact that the channel model used in the first example does not account for the transition-shifts inherent in the read back signal, whereas the second model does account for this.

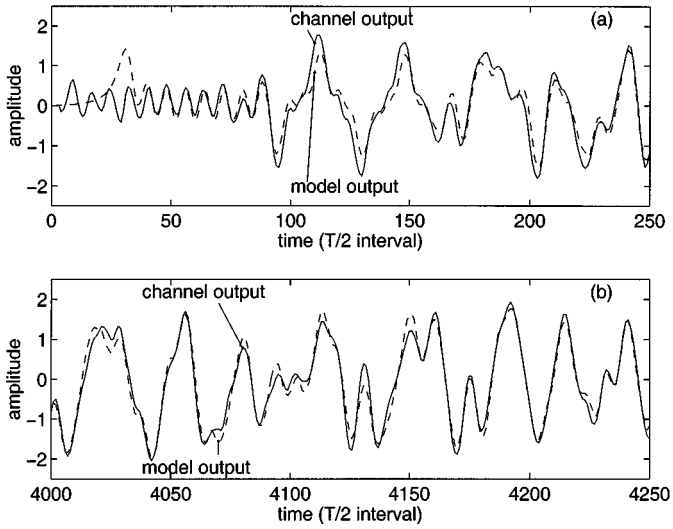

Fig. 3. Synchronous characterization for measured signal at density 4.9 using polynomial model.

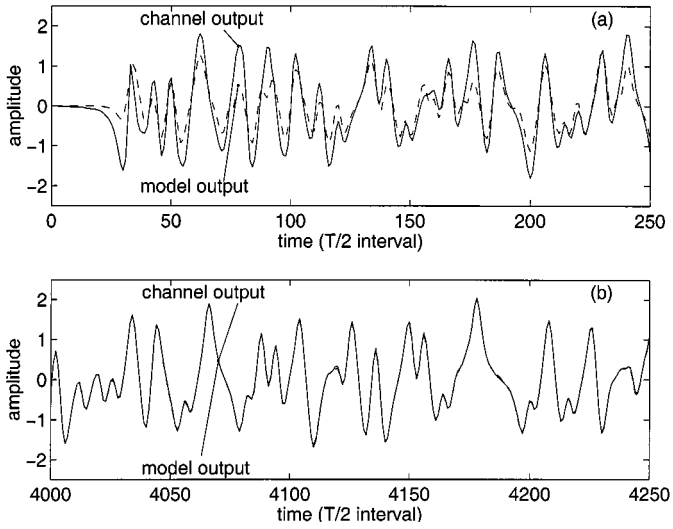

Fig. 4. Synchronous characterization for simulated signal at density 3.0 with data-dependent transition-shifts in the range $\{-0.4T, 0.4T\}$ using Volterra model.

The above results show that the proposed joint characterization and synchronization approach is robust and able to simultaneously provide accurate synchronization and characterization at high densities and in the presence of severe data dependent distortions.

REFERENCES

[1] D. Palmer, P. Ziperovich, R. Wood, and T. Howell, "Identification of nonlinear write effects using pseudorandom sequences," *IEEE Trans. Magn.*, vol. 23, no. 5, pp. 2377–2379, Sept. 1987.

[2] R. Hermann, "Volterra modeling of digital magnetic saturation recording channels," *IEEE Trans. Magn.*, vol. 26, no. 5, pp. 2125–2127, Sept. 1990.

[3] J. W. M. Bergmans, *Digital Baseband Transmission and Recording*. Norwell, MA: Kluwer Academic Publishers, 1996.